Electrical conduction mediated by fluorine atoms in the pyrochlore fluorides RbV_2F_6 and CsV_2F_6 with mixed-valent V atoms

Hiroaki Ueda,[1] Kihiro Yamada,[1,2] Hirotaka Yamauchi,[3] Yutaka Ueda,[3,4] and Kazuyoshi Yoshimura[1]

[1]*Department of Chemistry, Graduate School of Science, Kyoto University, Kitashirakawa Oiwake-cho, Sakyo-ku, Kyoto 606-8502, Japan*

[2]*Institute for Chemical Research, Kyoto University, Gokasho, Uji, Kyoto, 611-0011, Japan*

[3]*The Institute for Solid State Physics, The University of Tokyo, 5-1-5, Kashiwanoha, Kashiwa, Chiba 277-8581, Japan*

[4]*Toyota Physical and Chemical Research Institute, 41-1 Yokomichi, Nagakute, Aichi 480-1192, Japan*

(Received 31 March 2016; revised manuscript received 17 May 2016; published 31 May 2016)

We have investigated structural, electrical, and magnetic properties of single crystals of modified pyrochlore fluorides RbV_2F_6 and CsV_2F_6, which have mixed-valent V atoms. At room temperature, they have orthorhombic structures. With increasing temperature, each of them exhibits two structural transitions, and electrical resistivity rapidly decreases accompanied with one of these structural changes. The changes of unit cell volume and electrical resistivity at these transition temperatures indicate that the structural instability and the charge ordering cause structural transitions of RbV_2F_6 and CsV_2F_6, respectively. At low temperatures, CsV_2F_6 shows antiferromagnetic ordering at 5 K, and RbV_2F_6 shows two-step magnetic transitions.

DOI: 10.1103/PhysRevB.93.195168

I. INTRODUCTION

Most of fluorides are electrically insulating because of their strong ionic characteristics. The electron affinity of fluorine is the largest among those of all elements, and the chemical bonds between fluorine atoms and other kinds of atoms are highly ionic. Hence all electrons in a fluoride are localized around a fluorine atom or an atom bonded with fluorine atoms, and electrical conduction is suppressed. However, we have some exceptions that have low electrical resistivity: Hg_3NbF_6, Hg_3TaF_6 [1], and Ag_2F [2]. In their crystal structures, Hg or Ag atoms form layers with metal-metal bonds, which cause electrical conduction. Electron conduction mediated by fluorine atoms was not reported even in these electrically conducting fluorides.

On the other hand, many transition-metal oxides exhibit electrical conduction. Their electrical conduction is due to strong hybridization of oxygen p orbitals and transition-metal d orbitals. Particularly, most of mixed-valent oxides are electrically conducting, since the Fermi level is located in the middle of d bands. One of the most popular examples of mixed-valent oxides is magnetite Fe_3O_4. In the structure, Fe^{2+} and Fe^{3+} are distributed on a pyrochlore lattice, and charge frustration was discussed by Anderson [3]. Oxides with a mixed-valent state on a pyrochlore lattice include some spinels (LiV_2O_4 [4,5], AlV_2O_4 [6], $CuIr_2O_4$ [7]), and modified pyrochlores (CsW_2O_6 [8,9], AOs_2O_6 [10,11]), and most of them are electrically conducting.

Although there are some fluorides with mixed-valent ions, there are no detailed reports. One of such materials is the modified pyrochlore fluoride system. Modified pyrochlore fluorides have a chemical formula of $AMM'F_6$, where A is an alkaline metal, M is a divalent atom, and M' is a trivalent atom. [12]. Most of them contain two kinds of transition metals, M and M' [13]. Some of the modified pyrochlore fluorides have the same transition metal $M = M'$ such as AFe_2F_6 [14,15], ACr_2F_6 [15–17], and AV_2F_6 [16] (A = Rb and Cs), in which the formal valence of M is +2.5. In these compounds, divalent and trivalent cations are likely to order in a pyrochlore lattice, and hence they are electrically insulating. The former two systems AFe_2F_6 and ACr_2F_6 are undoubtedly insulating, because their colors are not black. However, AV_2F_6 was reported to be black, which indicates possible electrical conduction.

In this paper, we report the structural, electrical, and magnetic properties of modified pyrochlore fluorides RbV_2F_6 and CsV_2F_6. We found that they exhibit some structural transitions at high temperatures. Furthermore, they are electrically conducting, and show a jump in electrical resistivity with varying temperature. We discuss the origin of these transitions concerning the formation of charge orderings. In addition, both of them exhibit magnetic orderings at low temperatures, one of which has two-step feature.

II. EXPERIMENTAL DETAILS

Single crystals of AV_2F_6 (A = Rb and Cs) were grown using ACl-flux methods [18]. As starting materials, we used V grains and halides VF_3, AF, and ACl. We did not use V powder but V grains, since V powder gives low-quality samples owing to the presence of a certain amount of oxide formed on the surface of V powder. These halides had been dried or purified before use. These starting materials were mixed with an appropriate ratio, and were heated and slowly cooled in a Ni crucible. All above procedures were conducted in a glove box filled with Ar gas. The flux was removed using water.

X-ray diffraction measurements at high temperatures were conducted in a small furnace filled with He gas using a diffractometer with a Cu K_α source. The signals from Cu $K_{\alpha 2}$ were numerically subtracted from raw data. Electrical resistivities of single crystals at high temperatures were measured using a conventional four-probe method under an Ar atmosphere. Direct-current magnetization measurements were performed using commercial superconducting quantum interference device magnetometers (Quantum Design) in the Research Center for Low Temperature and Materials Sciences, Kyoto University. Specific heat measurements were carried out using a two-τ relaxation method (Quantum Design). In order

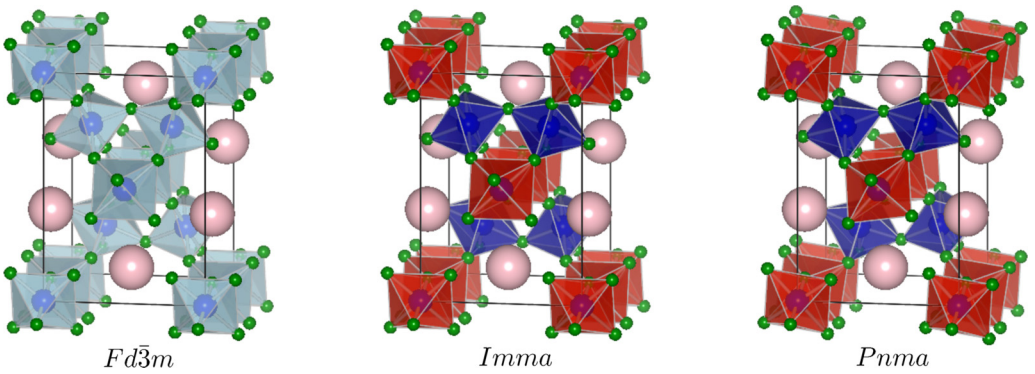

FIG. 1. Crystal structures of AV_2F_6 with space groups of $Fd\bar{3}m$, $Imma$, and $Pnma$ (spheres: A, octahedra: VF_6). The unit cells of orthorhombic $Imma$ and $Pnma$ structures, which are indicated by lines, are $1/\sqrt{2} \times 1/\sqrt{2} \times 1$ of the cubic $Fd\bar{3}m$ unit cell. While the cubic $Fd\bar{3}m$ structure has single V site, orthorhombic structures have two V sites, which is indicated using the colors of octahedra. The difference between the $Imma$ structure and the $Pnma$ structure is the rotation of VF_6.

to evaluate the lattice contributions, we measured the specific heats of nonmagnetic compound $AZnGaF_6$ with a cubic modified pyrochlore structure. The lattice specific heat at each temperature was compensated for by the Debye temperature θ_D, assuming that θ_D inversely proportional to the square root of the formula weight. Magnetic entropies were obtained from specific heats divided by temperature after the subtraction of the lattice contribution.

III. RESULTS AND DISCUSSIONS

The obtained single crystals of RbV_2F_6 and CsV_2F_6 are black and have octahedral shapes. A typical size of the crystal is approximately 2 mm in edge. The octahedral shapes suggest that RbV_2F_6 and CsV_2F_6 seem to be cubic when the crystal forms at high temperatures in the crystal growth. As mentioned below, owing to the transitions to the orthorhombic structure, six domains emerge in a single crystal, when the crystal is cooled down to room temperature. Our single crystals of RbV_2F_6 and CsV_2F_6 consist of crystallite domains, which prevent us from conducting structural analysis using single crystals. Hence powder x-ray diffraction measurements are important to elucidate the structural transitions of these compounds.

Powder x-ray diffraction patterns indicate that both RbV_2F_6 and CsV_2F_6 are orthorhombic at room temperature. However, the details of extinction rules of these two are different. The space groups of RbV_2F_6 and CsV_2F_6 are $Pnma$ and $Imma$, respectively. These space groups are consistent with a previous report [16]. It is noteworthy that $Pnma$ is a subgroup of $Imma$. Our x-ray investigations revealed that both RbV_2F_6 and CsV_2F_6 become cubic $Fd\bar{3}m$ at high temperatures as described below. In Fig. 1, the three crystal structures of modified pyrochlore with three space groups are displayed.

Figure 2 demonstrates temperature T dependence of the x-ray diffraction pattern of RbV_2F_6. At high temperatures, the pattern is consistent with the cubic modified pyrochlore structure, which has a space group of $Fd\bar{3}m$. Below 600 K, most of the diffraction signals split, which indicates a structural change. The splitting of the 220 signal indicates that the crystal system is not cubic, and the splitting of the 202 signal indicates that it is not tetragonal. The diffraction pattern just below 600 K suggests that the structure has an orthorhombic space group of $Imma$ with a $1/\sqrt{2} \times 1/\sqrt{2} \times 1$ unit cell compared with that of cubic phase. Below 540 K, the peak splittings become more distinct, and in addition, some diffraction signals such as 201 and 210 appear in orthorhombic indices. The presence of these new diffraction signals violate the extinction rule of $Imma$, and suggest that the space group becomes $Pnma$.

Although CsV_2F_6 also becomes cubic at high temperatures, the details of structural changes are different from those of

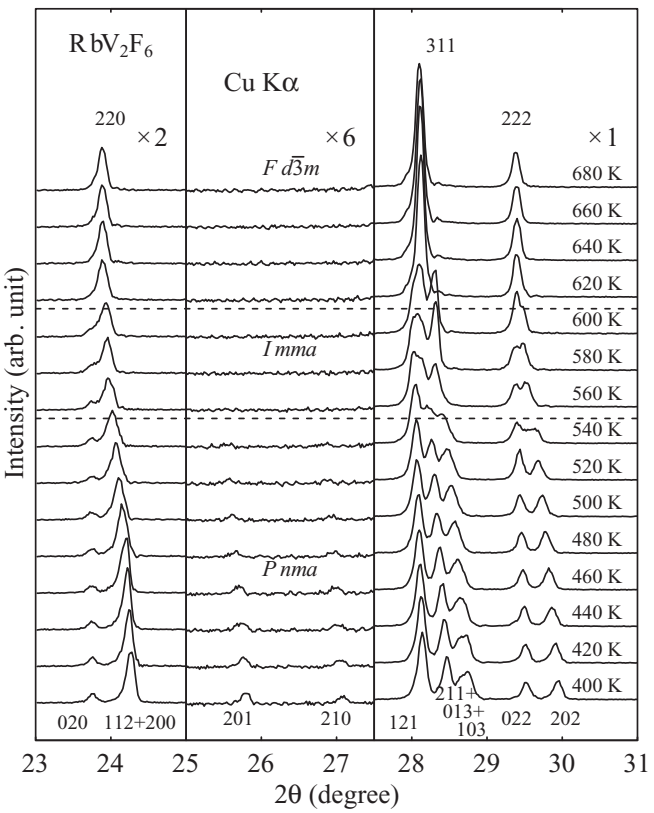

FIG. 2. Temperature dependence of the powder x-ray diffraction pattern of RbV_2F_6. To show the changes clearly, the intensities of $23^\circ \sim 25^\circ$ and $25^\circ \sim 27.5^\circ$ are enlarged by a factor 2 and 6, respectively. The broken lines indicate the boundary of the phases.

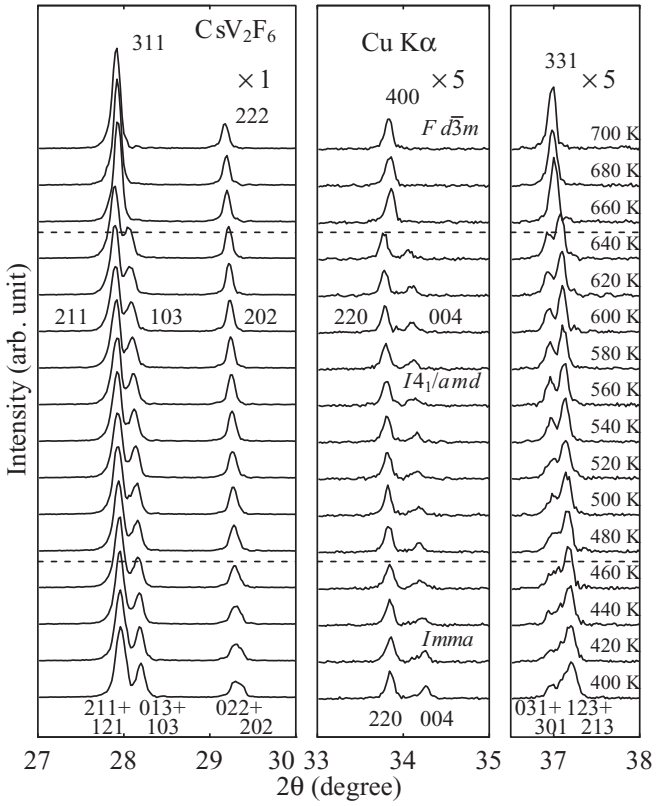

FIG. 3. Temperature dependence of the powder x-ray diffraction pattern of CsV_2F_6. To show the changes clearly, the intensities of $33^\circ \sim 35^\circ$ and $36.5^\circ \sim 38^\circ$ are enlarged by a factor 5. The broken lines indicate the boundary of the phases.

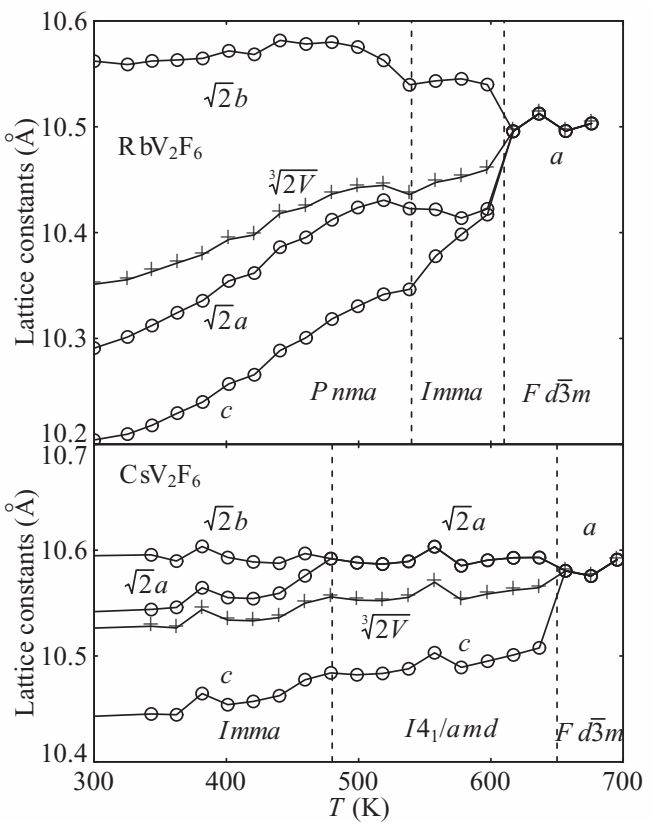

FIG. 4. The lattice constants and the unit cell volumes of RbV_2F_6 and CsV_2F_6 as a function of temperature. We note that a in the cubic unit cell corresponds to $\sqrt{2}a$, $\sqrt{2}b$, and $\sqrt[3]{2V}$ in the tetragonal or orthorhombic unit cell. The broken lines indicate the boundary of the phases.

RbV_2F_6 reflecting the difference in the space group at room temperature. Figure 3 demonstrates T dependence of the x-ray diffraction pattern of CsV_2F_6. As is the same as RbV_2F_6, the high-temperature pattern is consistent with the cubic modified pyrochlore structure. However, low-temperature structures are different from those of RbV_2F_6. Below 640 K, some diffraction signals split, which indicates a structural change to a tetragonal structure with a space group of $I4_1/amd$. No broadening of the 222 signal suggests that the system has $a = b$. Below 460 K, some diffraction signals, such as those at approximately 29.5° and 37°, become broader. These broadenings indicate that the value of a is not equal to that of b and that the space group becomes $Imma$. The peak splitting of x-ray diffraction pattern is less distinct than that of RbV_2F_6. No superlattice reflection was observed.

These structural changes are summarized as temperature dependencies of the lattice parameters as shown in Fig. 4, which clearly demonstrate the differences in structural transitions between RbV_2F_6 and CsV_2F_6. For RbV_2F_6, a, b, and c have the same value at high temperatures reflecting the cubic structure. With decreasing temperature, the lattice constants jump approximately at 600 K, indicating this structural transition is of first order. Please note that the unit cell of tetragonal phase is $1/\sqrt{2} \times 1/\sqrt{2} \times 1$ of that of cubic one. Slightly below the transition temperature, $\sqrt{2}a$ and c of the orthorhombic unit cell have almost the same value and the value of $\sqrt{2}b$ is substantially larger than those of them. With further decreasing temperature, $\sqrt{2}a$ and c gradually separate with each other, and the temperature dependence of lattice parameters has an anomaly at 560 K, indicating a second-order transition. At 300 K, the difference of the lattice parameters is more than 0.3 Å. In contrast, CsV_2F_6 has small difference of the lattice parameters at 300 K, which is approximately 0.15 Å. In addition, temperature dependence of the lattice constants in CsV_2F_6 is qualitatively different from that in RbV_2F_6. At high temperatures, a, b, and c have the same value. Approximately, at 650 K, c abruptly reduces, while the other two remain almost constant, which indicates the structure becomes tetragonal with a space group of $I4_1/amd$ through a first-order transition. Again, please note that the unit cell of tetragonal phase is $1/\sqrt{2} \times 1/\sqrt{2} \times 1$ of that of cubic one. Below 480 K, $\sqrt{2}a$ and $\sqrt{2}b$ gradually separate from each other and the system becomes an orthorhombic structure with a space group of $Imma$.

In addition to the difference in the space group at room temperature, one of the most significant differences between the structural changes of RbV_2F_6 and CsV_2F_6 is the directions of the lattice distortions. With decreasing temperature, the cubic $Fd\bar{3}m$ phase of RbV_2F_6 directly transforms into the $Imma$ phase with $\sqrt{2}b > \sqrt{2}a \sim c$. The cubic $Fd\bar{3}m$ phase of CsV_2F_6 goes into the $Imma$ phase with $\sqrt{2}b \sim \sqrt{2}a > c$ through the tetragonal $I4_1/amd$ phase. Although both

compounds have the $Imma$ phase, they have different tendencies: $\sqrt{2}a \sim c$ for RbV_2F_6 and $\sqrt{2}a \sim \sqrt{2}b$ for CsV_2F_6. These lattice constants indicate that the cubic crystal of RbV_2F_6 elongates along the [110] direction and that of CsV_2F_6 shrinks along the [001] directions in their $Imma$ phases. The different distorting directions of the $Imma$ phase indicate that the origins of the structural phase transitions of RbV_2F_6 and CsV_2F_6 are different.

Modified pyrochlore compounds have a large A-site ion, which means that the corner-sharing network of VF_6 octahedra have large holes at the A site. Structural instability owing to this large hole would be one possible origin of the structural transitions of AV_2F_6 compounds. Particularly, RbV_2F_6 has a smaller A-site ion and larger space around the ion than that of CsV_2F_6. The upper panel of Fig. 4 displays shrinkage along the $[1\bar{1}0]$ and [001] direction, expansion along the [110] direction in the cubic indices, and volume reduction, accompanied with the structural transition from $Fd\bar{3}m$ to $Imma$. These changes indicate that the large space around A ion is closely related to this structural transitions of RbV_2F_6. The slight volume increase with structural transition from $Imma$ to $Pnma$ of RbV_2F_6 is possibly due to the rotation of VF_6 octahedra in the $Pnma$ structure. In contrast, the lower panel of Fig. 4 displays that CsV_2F_6 exhibits a small volume change accompanied with structural transitions, suggesting that the space around A ion has little effect on the structural transitions of CsV_2F_6.

In addition to the large hole mentioned above, charge ordering would be another likely origin of structural transitions, particularly for CsV_2F_6. RbV_2F_6, and CsV_2F_6 have V atoms with a formal valence of +2.5. It is likely that charge orderings of V^{2+} and V^{3+} take place with the change of structure. If the charge orderings take place, the number of V sites would become two or more. In the cubic $Fd\bar{3}m$ structure, corner-sharing VF_6 chains along $\langle 110 \rangle$ are equivalent. Although the structure shrinks along the c direction in the tetragonal $I4_1/amd$ structure of CsV_2F_6, the chains along [110] and $[1\bar{1}0]$ in the cubic indices are equivalent as shown in Fig. 1. Hence the cubic $Fd\bar{3}m$ and tetragonal $I4_1/amd$ structures have a single V site, indicating no charge ordering. In contrast, these two kinds of chains expand or shrink in the $Imma$ structure, and VF_6 octahedra rotate in the $Pnma$ structure of RbV_2F_6, and therefore orthorhombic $Imma$ and $Pnma$ structures have two V sites as shown in Fig. 1. In the charge ordering states of $Imma$ and $Pnma$ structures, V^{3+} ions with $S = 1$ form one-dimensional chains along the $[1\bar{1}0]$ direction, and V^{2+} ions with $S = 3/2$ form those along the [110] direction, where cubic indices are used. Please note that all V_4 tetrahedra consist of two V^{2+} and V^{3+}, which satisfies the Anderson's criteria of charge ordering in a pyrochlore lattice [3]. In our structural study of RbV_2F_6 mentioned above, the number of V sites changes from one to two owing to the structural transition from $Fd\bar{3}m$ to $Imma$ approximately at 600 K. For CsV_2F_6, it changes owing to the transition from $I4_1/amd$ to $Imma$ approximately at 480 K.

Charge ordering is closely related to the electron transfer from one V ion to another one. This means that the formation of charge ordering has large effects on electrical resistivity. Although most of fluorides are electrically insulating, black colors of RbV_2F_6 and CsV_2F_6 indicate possible electron conduction.

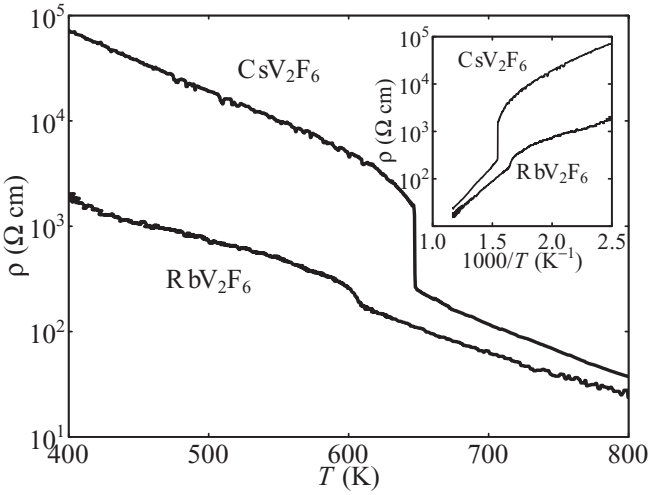

FIG. 5. Temperature dependence of electrical resistivities of RbV_2F_6 and CsV_2F_6. The main panel shows ρ-T curves. At high temperatures, the values of ρ of RbV_2F_6 and CsV_2F_6 are of the order of 10^2 Ωcm. In the entire temperature range, ρ exhibits semiconducting temperature dependence.

Figure 5 shows T dependence of electrical resistivities ρ of RbV_2F_6 and CsV_2F_6 measured at high temperatures. Surprisingly, electrical conduction is observed in these fluorides, although the values of ρ are high. For both compounds, ρ gradually decreases with increasing T. Approximately at 650 K, ρ of CsV_2F_6 suddenly drops by one order of magnitude, indicating an electronic phase transition. In contrast, RbV_2F_6 exhibits small change of ρ approximately at 600 K. With further increasing T, ρ gradually decreases again for both compounds.

The jump of ρ approximately at 650 K observed for CsV_2F_6 suggests that this transition is caused by charge ordering of V^{2+} and V^{3+}. However, above-mentioned structural study suggests that this transition corresponds to the structural transition from $Fd\bar{3}m$ to $I4_1/amd$ with a single V site, and the number of V sites does not seem to change through this structural transition. The number of V sites is two in the $Imma$ phase observed below 480 K, and there is no anomaly in ρ at this temperature. It is natural to think that the electronic state of the $I4_1/amd$ phase is similar to that of the $Imma$ phase. Hence we think that the $I4_1/amd$ phase has a very small orthorhombic distortion and that it has two V sites, which correspond to V^{2+} and V^{3+}.

For RbV_2F_6, the jump of ρ approximately at 600 K is very small compared with that of CsV_2F_6. This temperature corresponds to the structural transition from $Fd\bar{3}m$ with a single V site to $Imma$ with two V sites, which is consistent with the charge ordering scenario. However, the change of ρ at the transition temperature is much smaller than that of CsV_2F_6. In the structural view point, the most significant difference between RbV_2F_6 and CsV_2F_6 is the changes of lattice constants at their transition temperatures, which are shown in Fig. 4. For CsV_2F_6, the change of lattice constants is very small, indicating that V–V distances below and above the transition temperature are almost the same. Owing to charge ordering, electrons on V ions are localized and ρ drastically increases. In contrast, for RbV_2F_6, V–V

distances along the b axis are large and others are small in the orthorhombic structure below the transition temperature. Particularly, substantial contraction is observed in V chains along [112] in the orthorhombic index consisting of V^{2+} and V^{3+}. The reduction of the V–V distance enhances electron transfer between V^{2+} and V^{3+}, which is likely to reduce ρ in the charge ordering state. Hence the jump of ρ is small for RbV_2F_6.

To elucidate the origin of electron transfer from one V atom to a neighboring one through F atoms bridging between them, we plot $\log_{10}\rho$ as a function of $1/T$ in the inset of Fig. 5. In the high-temperature cubic phase, the linear behaviors suggest that ρ is described as the activation type resistivity $\rho = \rho_\infty \exp(E_a/k_BT)$, where E_a is the activation energy, and k_B is the Boltzmann constant. The activation energies E_a of CsV_2F_6 and RbV_2F_6 are approximately 0.54 and 0.43 eV, respectively. The lower activation energy of RbV_2F_6 is due to the shorter V–V distances in the cubic phase. These gap energies are consistent with the fact that both compounds are black in color. The values of ρ_∞ are 0.0146 and 0.015 Ω cm for CsV_2F_6 and RbV_2F_6, respectively. In the low-temperature phase, however, the data become noisy and have sample dependence (not shown here), which are possibly owing to the domain formation. Below the transition temperatures, $\log_{10}\rho$-$1/T$ plots are not linear, indicating the change of mechanism of electron transport owing to the formation of charge ordering. In charge ordering systems, variable range hopping is sometimes discussed. However, variable range hopping type plots are not linear for low temperature phases of AV_2F_6. To compare the transport behaviors above and below transition temperature, we will discuss $\log_{10}\rho - 1/T$ plots also in low-temperature phases. In the low-temperature phase, ρ_∞ is larger and E_a is smaller than those of the high-temperature phase for each compound. The obtained parameters at low temperatures for CsV_2F_6 are $\rho_\infty = 30\ \Omega$ cm and $E_a = 0.27$ eV, and those for RbV_2F_6 are $\rho_\infty = 10\ \Omega$ cm and $E_a = 0.18$ eV. With the formation of charge orderings, ρ_∞ becomes large. The V–V distance of RbV_2F_6 is much smaller than that of CsV_2F_6 at low temperatures, which is likely to cause the difference of ρ_∞ at low temperatures. It seems strange that the values of E_a at low temperatures are smaller than those at high temperatures. The resistivity is mainly governed by the carrier density and the mobility of the carriers. The temperature dependence of lattice parameters shown in Fig. 4 suggests that the V–V distance and the mobility of the carriers strongly depend on the temperature especially below the transition temperatures. This T dependence of mobility is likely to violate the activation law, and the values of E_a seem to reduce. The fact that ρ strongly depends on –V distances, indicates that the electron conduction between V atoms is enhanced by the orbital overlapping of V atoms and F atoms bridging between them.

In addition to ρ, the magnetic susceptibility χ gives information about the electronic state of V atoms, since the change of the electronic state affects the spin state. For RbV_2F_6 and CsV_2F_6, temperature dependencies of χ are shown in Fig. 6. As shown in the right inset of Fig. 6, χ data measured under 1 T in both compounds are well-fitted using the Curie-Weiss law except for low-temperature regions. The values of effective magnetic moments $p_{\rm eff}$ are 3.21 ± 0.06 and 3.35 ± 0.03, and the Curie-Weiss temperatures Θ are -19.5 ± 0.4 K and 0.7 ± 0.3 K for RbV_2F_6 and CsV_2F_6, respectively. The experimentally obtained values of $p_{\rm eff}$ are quite consistent with the ideal value of 3.39, which is the root-mean-square of $p_{\rm eff}$ of V^{3+} with $S = 1$ and V^{2+} with $S = 3/2$ assuming $g = 2$. This fact suggests that these magnetic systems are well-described as 1:1 mixtures of V^{3+} and V^{2+}.

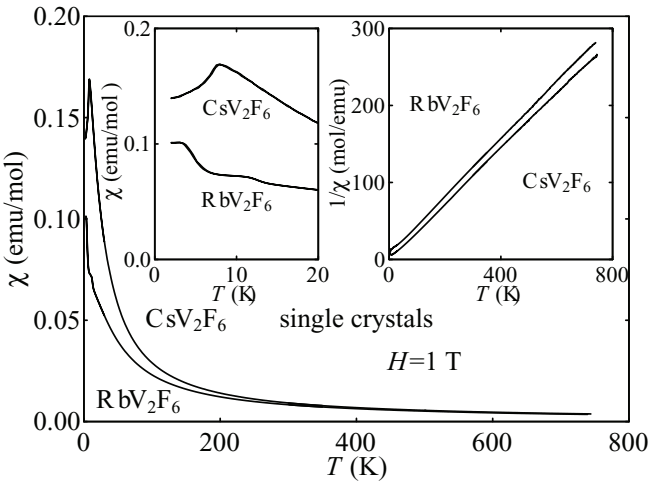

FIG. 6. Temperature dependence of magnetic susceptibility χ of RbV_2F_6 and CsV_2F_6. Inverse magnetic susceptibility $1/\chi$ data are plotted in the inset. These measurements are conducted using single crystals with random orientation.

It is noteworthy that the slope of the $1/\chi - T$ plot does not change at the temperature where ρ jumps for each compound, suggesting that the spin states of V below and above the transition temperature are quite similar. Below the transition temperature, electrons of V^{2+} and V^{3+} are localized and V^{2+} and V^{3+} are ordered. Even above the transition temperature, the $p_{\rm eff}$ is larger than the ideal value of $p_{\rm eff}$ for the valence of +2.5, which is 2.96. At the transition temperature, the slope of $1/\chi - T$ does not change, and the $p_{\rm eff}$ is larger than the ideal value of $p_{\rm eff}$ for the valence of +2.5, which is 2.96. Although electrons transfer among V atoms at high temperatures, $p_{\rm eff}$ suggests that the valence of V is not +2.5 but a mixture of +2 and +3. It is likely that V^{2+} and V^{3+} are randomly distributed and their electrons transfer among them.

At room temperature, V^{2+} and V^{3+} are ordered for both compounds. At low temperatures, their spins exhibit magnetic orderings. As shown in the left inset of Fig. 6, $\chi - T$ curves of both compounds exhibit anomalies at low temperatures. However, these anomalies have remarkable difference between two compounds. For CsV_2F_6, the anomaly of χ at $T_{\rm N} \approx 8$ K is similar to those of conventional antiferromagnetically ordered systems. In contrast, χ of RbV_2F_6 increases stepwise at $T_{\rm N1} \approx 13$ K and $T_{\rm N2} \approx 6$ K with decreasing temperature.

To elucidate the origin of the two-step magnetic transition of RbV_2F_6, we have measured the magnetic field, H, dependence of the magnetization M and we plot M/H-T as shown in the left inset of Fig. 7. Two magnetically ordered phases of RbV_2F_6 have ferromagnetic characteristics. At 7 T, two anomalies at $T_{\rm N1}$ and $T_{\rm N2}$ are not distinct in M/H. With decreasing magnetic field, M/H below $T_{\rm N2} \approx 6$ K gradually increases, which suggests the existence of spontaneous

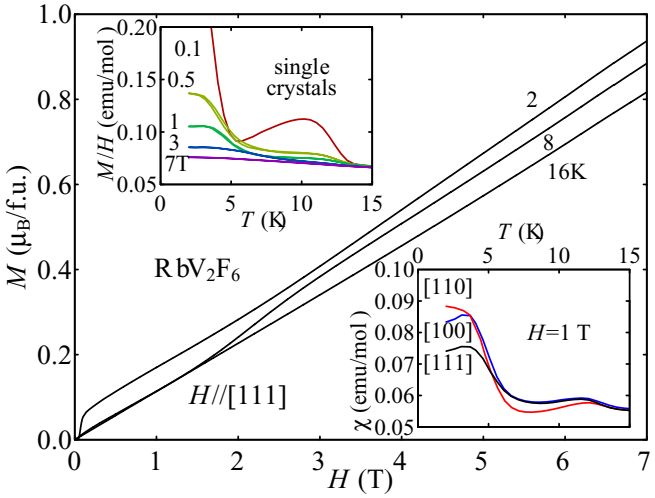

FIG. 7. Magnetization of RbV_2F_6 per formula unit as a function of magnetic field at various temperatures. After cooling under zero field condition, these measurements were conducted with increasing magnetic field. In the left inset, M/H is plotted as a function of temperature under various magnetic fields, which were measured in field cooled conditions. In the right inset, χ data measured under magnetic fields with various directions are shown. The directions of the field were indexed based on the cubic system. Owing to the orthorhombic domain formation in a single crystal, cubic [100] corresponds to orthorhombic [001], [110], and [1$\bar{1}$0] directions. Similarly, cubic [110] corresponds to orthorhombic [100], [010], and [112] directions. Cubic [111] corresponds to orthorhombic [101] and [011] directions.

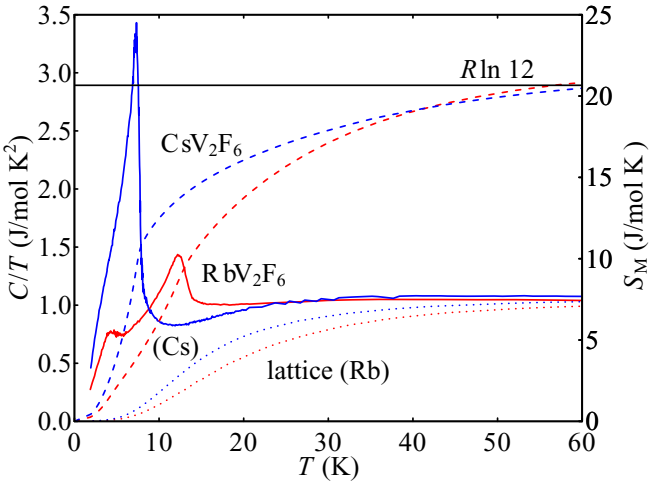

FIG. 8. Specific heat divided by temperature C/T (solid lines) and magnetic entropy S_M (dashed lines) of RbV_2F_6 and CsV_2F_6 as a function of temperature. The lattice contribution estimated from the specific heat of $RbZnGaF_6$ or $CsZnGaF_6$ (dotted lines) is used to calculate S_M.

magnetization. The field dependence of M/H between T_{N1} and T_{N2} is small, but the step at $T_{N1} \approx 13$ K is pronounced below 0.1 T.

To determine the direction of spins in the magnetically ordered phases, the direction dependence of χ-T is measured as shown in the right inset of Fig. 7. In general, the phase with spontaneous magnetization has large direction dependence of $\chi = M/H$. However, three χ-T curves of $H \parallel$ [100], [110], and [111] are different but similar to that of randomly oriented single crystals in Fig. 6. This similarity is likely due to the domain formation in the single crystal as mentioned before. A single direction in the cubic phase corresponds to several orthorhombic directions. Even if the magnetic measurements are conducted using a single crystal in cubic condition, the data come from six orthorhombic domains. Hence M of a single crystal with domain formation is similar to that of the polycrystalline samples.

In Fig. 7, M-H curves of $H \parallel$ [111] at various temperatures are exhibited. In the paramagnetic phase at 16 K ($>T_{N1}$), the M-H curve is linear. At 8 K ($<T_{N1}$), M linearly increases up to 1.5 T, and rapidly increases around 2 T, and again increases linearly. At 2 K ($<T_{N2}$), M jumps to 0.05 μ_B in the low-field region, indicating the ferromagnetic nature, and the M-H curve slightly bends approximately at 2 T. From these measurements, the difference between two magnetically ordered phases is clarified. Below T_{N2}, RbV_2F_6 is in a canted antiferromagnetic phase with small spontaneous magnetization. Between T_{N2} and T_{N1}, it is in an antiferromagnetic phase with a spin-flop transition approximately at 2 T.

For CsV_2F_6, $T_N = 8$ K is approximately half of $|\Theta| = 20$ K. However, for RbV_2F_6, $T_{N1} = 13$ K is much higher than $|\Theta| = 1$ K. The value of Θ scales the average of various magnetic interactions J between V spins. In the orthorhombic structure, there are several neighboring V–V bonds. If the magnetic interactions of them have different signs, T_N possibly becomes much higher than $|\Theta|$.

Compared with CsV_2F_6, RbV_2F_6 has a crystal structure with lower symmetry, which means that RbV_2F_6 has many kinds of neighboring V–V interactions. The *Imma* structure of CsV_2F_6 has three kinds of neighboring V–V bonds, V^{2+}–V^{2+}, V^{3+}–V^{3+}, and V^{2+}–V^{3+}. While the *Pnma* structure of RbV_2F_6 has four –V bonds, V^{2+}–V^{2+}, V^{3+}–V^{3+}, and two V^{2+}–V^{3+}. Many kinds of neighboring J of RbV_2F_6 seemingly make nearly degenerated magnetic structures and a two-step magnetic transition.

Accompanied by the formation of magnetic ordering, the change in the magnetic entropy S_M occurs. To evaluate S_M, we measured the specific heats C of RbV_2F_6 and CsV_2F_6. In Fig. 8, the temperature dependence of C/T and S_M is displayed.

For CsV_2F_6, C/T exhibits a lambda-type anomaly at T_N, and then remains almost constant above T_N. The sharp lambdalike feature in C/T suggests that long-range ordering is established at this temperature. For RbV_2F_6, two lambda-type anomalies are observed at T_{N1} and T_{N2}.

Magnetic entropies S_M of CsV_2F_6 and RbV_2F_6 rapidly increase at T_N, T_{N1}, and T_{N2} reflecting the variation of C/T, and continue to increase above them. The total magnetic entropy, which is the sum of the $R\ln(2S+1)$ values of V^{2+} ($S = 3/2$) and V^{3+} ($S = 1$), equals $R\ln 12 \approx 20$ J/mol K. Up to 60 K, S_M of both compounds reach approximately the total magnetic entropy. These observations suggest that only the magnetic degree of freedom remains below 60 K for these compounds, and that charge and orbital degrees of freedom

are already relieved. This is consistent with our conclusion that the charge ordering takes place at high temperatures.

IV. SUMMARY

Our experiments revealed that two mixed-valent modified pyrochlore fluorides RbV_2F_6 and CsV_2F_6 are electrically conducting, although the temperature dependence of resistivities of these compounds are semiconducting. Accompanied by a structural transition indicating the formation of charge orderings of V^{2+} and V^{3+}, the resistivity of each compound abruptly increases. In this charge ordering state, all V_4 tetrahedra contain two V^{2+} and V^{3+}. These vanadium ions are antiferromagnetically coupled, which is indicated by the negative values of Θ. At low temperatures, both systems exhibit magnetic orderings. Particularly, RbV_2F_6 exhibits two-step magnetic transitions.

ACKNOWLEDGMENTS

This work was supported by a Grant-in-Aid for Scientific Research (C) (Grant No. 24540345) from the Japan Society for the Promotion of Science.

[1] W. R. Datars, K. R. Morgan, and R. J. Gillespie, Phys. Rev. B **28**, 5049 (1983).
[2] H. Kawamura, I. Shirotani, and H. Inokuchi, Chem. Phys. Lett. **24**, 549 (1974).
[3] P. W. Anderson, Phys. Rev. **102**, 1008 (1956).
[4] S. Kondo, D. C. Johnston, C. A. Swenson, F. Borsa, A. V. Mahajan, L. L. Miller, T. Gu, A. I. Goldman, M. B. Maple, D. A. Gajewski, E. J. Freeman, N. R. Dilley, R. P. Dickey, J. Merrin, K. Kojima, G. M. Luke, Y. J. Uemura, O. Chmaissem, and J. D. Jorgensen, Phys. Rev. Lett. **78**, 3729 (1997).
[5] C. Urano, M. Nohara, S. Kondo, F. Sakai, H. Takagi, T. Shiraki, and T. Okubo, Phys. Rev. Lett. **85**, 1052 (2000).
[6] K. Matsuno, T. Katsufuji, S. Mori, Y. Moritomo, A. Machida, E. Nishibori, M. Takata, M. Sakata, N. Yamamoto, and H. Takagi, J. Phys. Soc. Jpn. **70**, 1456 (2001).
[7] T. Hagino, T. Tojo, T. Atake, and S. Nagata, Phil. Mag. B **71**, 881 (1995).
[8] R. J. Cava, R. S. Roth, T. Siegrist, B. Hessen, J. J. Krajewski, and W. F. Peck, Jr., J. Solid State Chem. **103**, 359 (1993).
[9] D. Hirai, M. Bremholm, J. M. Allred, J. Krizan, L. M. Schoop, Q. Huang, J. Tao, and R. J. Cava, Phys. Rev. Lett. **110**, 166402 (2013).
[10] S. Yonezawa, Y. Muraoka, Y. Matsushita, and Z. Hiroi, J. Phys. Soc. Jpn. **73**, 819 (2004).
[11] M. Brühwiler, S. M. Kazakov, N. D. Zhigadlo, J. Karpinski, and B. Batlogg, Phys. Rev. B **70**, 020503(R) (2004).
[12] E. Banks, J. A. Deluca, and O. Berkooz, J. Solid State Chem. **6**, 569 (1973).
[13] M. J. Harris, M. P. Zinkin, Z. Tun, B. M. Wanklyn, and I. P. Swainson, Phys. Rev. Lett. **73**, 189 (1994).
[14] S. W. Kim, S.-H. Kim, P. S. Halasyamani, M. A. Green, K. P. Bhatti, C. Leighton, H. Das, and C. J. Fennie, Chem. Sci. **3**, 741 (2012).
[15] W. O. J. Boo, R. F. Williamson, K. N. Baker, and Y. S. Hongba, Mol. Cryst. Liq. Cryst. **107**, 195 (1984).
[16] Y.-K. Yeh, Y.-S. Hong, W. O. J. Boo, and D. L. Mattern, J. Solid State Chem. **178**, 2191 (2005).
[17] H. Ueda, A. Matsuo, K. Kindo, and K. Yoshimura, J. Phys. Soc. Jpn. **83**, 014701 (2014).
[18] B. J. Garrard and B. M. Wanklyn, J. Cryst. Growth **47**, 159 (1979).